Progress In Electromagnetics Research B, Vol. 13, 111–131, 2009

DESIGN AND ANALYSIS CONSIDERATIONS OF 4 GHz INTEGRATED ANTENNA WITH NEGATIVE RESISTANCE OSCILLATOR

S. H. Ibrahim

Computer and Electronics Engineering Department
College of Applied Studies & Community Service
King Faisal University
P. O. Box 400, Al-Ahsa, K.S.A.

Abstract—The purpose of this paper is to present a complete design and analysis of a new integrated balanced transmitter operated at 4 GHz using microstrip technology. It comprises a 4 GHz two-port negative resistance oscillator and a microstrip-patch antenna resonated at 4 GHz. Three different modules are designed and analyzed. The first one used a Lange coupler as a power splitter while the second and third used a one (two)-section branch coupler. The components of the three modules are designed using full-scale computer simulation program named with MSDES, performed by the author, which fully takes into account all the discontinuities included in the microstrip lines, while the modules are analyzed and optimized using APLAC V7.61 software. The design methodologies of the two-port negative resistance oscillator and microstrip patch antenna are introduced and explained. The analyses of the designed modules show a better efficiency and good performance. The modules give a transmit-antenna gain of 15.7 dB with antenna beam widths 91.7° and 18.2° in E- and H-planes, respectively. The complete schematic diagrams of the transmitter modules are drawn. These modules can be used in satellite communications, Doppler and other radars, active and semi-active seekers, radio altimeters, missile technology, weapon fuzing, manpack equipments, remote sensing, feed elements in complex antennas, satellite navigation receivers, and biomedical radiators.

Corresponding author: S. H. Ibrahim (saidhassan1@yahoo.com).

1. INTRODUCTION

An active antenna integrates an active device (microwave diodes or transistors) into a printed antenna to improve its performance or combine functions within the antenna itself. Therefore, complete transmitter modules can be implemented in a single substrate. Such modules are of increasing interest, as system designers require more complex functions to be implemented in a reduced space [1–6]. The microstrip antennas are low profile, conformable to planar and nonplanar surfaces, simple and inexpensive to manufacture using modern printed-circuit technology, mechanically robust, and compatible with MMIC designs. The application of active antennas comprises active and semi-active seekers, remote sensors, collision avoidance radars, wireless local-area networks, etc.

The transmitter modules designed and presented in this paper comprises a negative resistance oscillator operated at a frequency of 4 GHz, a microstrip patch antenna resonant at 4 GHz, and Lange/branch coupler as power splitters. The modules are designed using the microstrip-line technology (relative permittivity $\varepsilon_r = 2.2$, dielectric thickness $H = 0.7874$ mm, and conductor thickness $t = 0.005$ mm) with the aid of the full-scale computer simulation program named by MSDES, performed by the author [7, 9], and analyzed using the APLAC V7.61 software.

The MSDES program is a visual user-oriented comprehensive computational program. The first published version was written by FORTRAN language [7] while the modified published version is written with Visual-basic language [8, 9]. The program can be used for a wide range of microstrip, coaxial, and waveguide applications. For microstrip applications it is used for active and passive circuits design such as microstrip amplifiers, oscillators, couplers, mixers and MPA taking fully into account all the discontinuities the microstrip design [10, 12]. For waveguide applications, it is used for the design of rectangular waveguide oscillators and amplifiers with post and disc assembly used for the tuning of the active element (IMPATT or Gunn diode). For coaxial applications, it is used for the design of coaxial amplifiers and oscillators with the design of the tuning circuit of the active element.

2. DESIGN OF 4 GHz NEGATIVE RESISTANCE TRANSISTOR OSCILLATOR

Microwave oscillator is a one-port device whose purpose is to provide stable sinusoidal signal to the microwave system in which it is

embedded. The oscillator must have a negative real part of the equivalent impedance under certain DC biasing [4, 10, 13, 16].

An oscillator consists of two elements: An active element and a passive element. The active element converts dc power to RF power. It is a solid-state device, a semiconductor-based transistor, or RF diode. The passive element serves three purposes: 1) It provides the necessary dc bias for the device to operate, 2) It presents an electromagnetic environment at the device's terminals to initiate oscillation, optimizes the oscillator's output power and efficiency, and shapes its frequency spectrum, and 3) It provides a stable thermal environment.

Compared with the one-port oscillator, The two-port (3-terminal) negative resistance oscillators have the advantages of more efficient, lower noise figure, and the input and output circuits are inherently isolated.

When a two-port device such as BJT or FET is used in the oscillator design, a terminating circuit (single/balanced open/short stub is loaded to the transistor to achieve the negative resistance at the desired frequency band. Moreover, a negative feedback stub is added to the base/gate terminal of the transistor to enhance the transistor instability through increasing the value of S_{11}.

Figure 1 shows the equivalent circuit of the negative resistance oscillator, where $Z_d(A, \omega)$ is the impedance of the active device including the terminating and feedback circuits, $Z_L(\omega)$ is the impedance of the passive load, A is the amplitude of the current in the loop ($I = A \cdot e^{j\omega t}$), and ω is the angular frequency. The circuit in Figure 1 is then described with:

$$[Z_d(A, \omega) + Z_L(\omega)] \cdot I = 0 \tag{1}$$

The process of the oscillation depends on the active element and the behavior of the nonlinear parameters of Γ_d in addition to the proper selection of the load termination Γ_L [11, 12]. When the oscillations exist in the circuit, the current cannot be zero ($I \neq 0$). As [1] is valid,

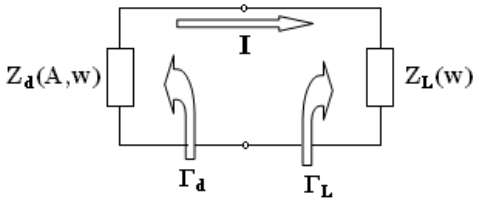

Figure 1. The equivalent circuit of a two-port negative resistance oscillator.

the value of $Z_d(A,\omega) + Z_L(\omega)$ must equal to zero, which results in:

$$Z_L(\omega) = -Z_d(A) \tag{2}$$

The design methodology of the two-port negative resistance oscillator has mainly four steps. The first step is the selection of the proper active element (BJT or FET) for the oscillation application. The Common-base HXTR-4101 BJT is used as an active element with the small-signal $[S]$ parameters shown in Table 1.

Table 1. Small-signal $[S]$ parameters of HXTR-4101 BJT.

HXTR 4101 *S*-PARAMETERS: Vc=15 V IC=30mA ta= 25 deg								
F	S_{11}		S_{21}		S_{12}		S_{22}	
GHz	MAG	ANG	MAG	ANG	MAG	ANG	MAG	ANG
1.0	0.93	161	1.93	–29	0.011	127	1.01	–15
1.5	0.94	153	1.92	–44	0.023	126	1.04	–31
2.0	0.96	144	1.95	–59	0.039	120	1.06	–45
2.5	0.98	134	1.97	–76	0.061	113	1.10	–59
3.0	0.99	123	1.96	–94	0.086	105	1.12	–74
3.5	1.01	115	1.95	–144	0.117	93	1.16	–91
4.0	1.02	106	1.87	–133	0.154	84	1.19	–108
4.5	1.01	96	1.79	–155	0.186	70	1.20	–127
6.0	0.91	74	1.32	144	0.245	35	1.10	–176
7.0	0.85	61	1.06	109	0.267	17	0.99	157
8.0	0.78	49	0.87	74	0.298	1	0.89	135
9.0	0.76	44	0.76	60	0.238	–10	0.93	131
10.0	0.72	27	0.72	29	0.288	–24	0.89	113

The stability of the used transistor at the frequency of 4 GHz is calculated through calculation of the stability factor, K, and Δ is given by [10, 15, 17]:

$$K = \frac{1 - |S_{11}|^2 - |S_{22}|^2 + |\Delta|^2}{2\,|S_{12}S_{21}|} \tag{3}$$

$$\Delta = S_{11}S_{22} - S_{12}S_{21} \tag{4}$$

Using the MSDES full-scale computer simulation program, the BJT is potentially unstable at the operating frequency of 4 GHz with $K = -0.6546$, $\Delta_{MAG} = 1.039$, and $\Delta_{ANG} = 9.696$.

The second step is to calculate the tuning element (open/short stub) at the base terminal of the active element to get maximum instability, maximizing S_{11}, at the desired operating frequency. Using MSDES design simulation program and the APLAC V7.61 software, the optimum length and width of the tuning open-circuit single stub at the base terminal of the active element are 16 mm and

2.408 mm respectively. Table 2 shows the new $[S]$ parameters of the active element with the tuning open-circuit stub at its base terminal. Figures 2 through 5 show S_{11}, S_{12}, S_{21}, S_{22}, Z_d, and Γ_d over the range 0–10 GHz for the active element with tuning stub. It is seen that S_{11} is increased to 1.25 and the circuit has a negative resistance over the range 3.35–4.45 GHz. In this range the values of Γ_d are greater than 1.

Table 2. Small-signal $[S]$ parameters of HXTR-4101 BJT with the tuning open stub at its base terminal.

HXTR 4101 *S*-PARAMETERS: Vc=15 V IC=30mA ta= 25 deg								
F	S_{11}		S_{21}		S_{12}		S_{22}	
GHz	MAG	ANG	MAG	ANG	MAG	ANG	MAG	ANG
1.0	0.27	162.35	1.27	–19.75	0.244	–7.98	0.76	–7.66
1.5	0.34	158.02	1.33	–29.31	0.298	–13.68	0.73	–17.19
2.0	0.42	149.79	1.42	–41.68	0.27	–21.766	0.76	–26.75
2.5	0.54	141.70	1.560	–58.19	0.209	–29.64	0.86	–40.26
3.0	0.76	129.21	1.77	–82.33	0.071	–33.956	1.005	–61.59
3.5	1.110	104.92	1.99	–156.05	0.219	91.25	1.134	–101.01
4.0	1.25	72.06	1.615	176.64	0.580	54.62	1.068	–158.42
4.5	0.965	46.39	0.964	118.47	0.66	23.03	0.69	148.7
6.0	0.52	30.20	0.61	8.53	0.63	–10.5	0.42	57.034
7.0	0.42	27.708	0.65	–35.734	0.63	–25.53	0.496	12.08
8.0	0.20	47.16	0.90	–86.90	0.64	–44.13	0.73	–44.51
9.0	0.627	100.27	1.40	–170.5	0.32	–86.62	1.26	–127.19
10.0	0.84	59.54	1.02	105.731	0.285	15.796	0.96	154.01

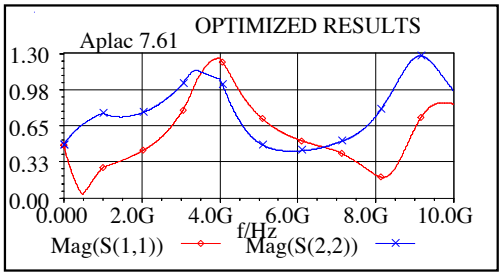

Figure 2. $|S_{11}|$ and $|S_{22}|$ versus frequency for the HXTR-4101 BJT with tuning stub at its base terminal.

The third step is the design and optimization of the oscillator terminating circuit so as to get negative input impedance at the desired operating frequency. Using MSDES simulation program and the APLAC V7.61 software, the optimum length and width of the terminating circuit at the emitter terminal of the active element

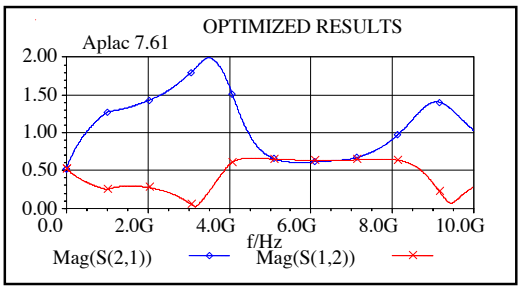

Figure 3. $|S_{21}|$ and $|S_{12}|$ versus frequency for the HXTR-4101 BJT with tuning stub at its base terminal.

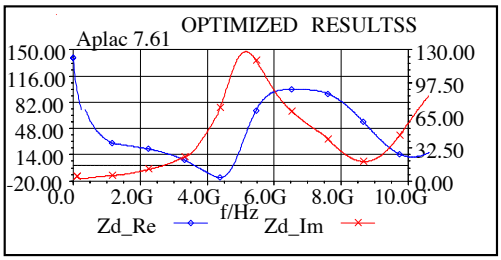

Figure 4. Real and imaginary parts of Z_d versus frequency for the HXTR-4101 BJT with tuning stub at its base terminal.

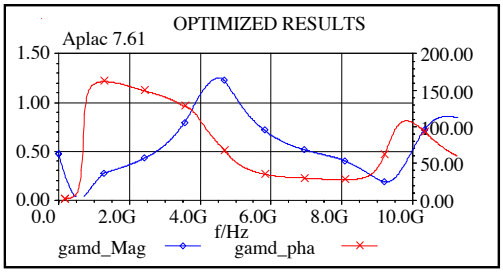

Figure 5. Magnitude and phase parts of Γ_d versus frequency for the HXTR-4101 BJT with tuning stub at its base terminal.

are 5.018 mm and 2.022 mm respectively. Figure 6 shows the Aplac configuration of the active element with the tuning and terminating open stubs at its base and emitter terminals. Figures 7 through 10 show S_{11}, S_{12}, S_{21}, S_{22}, Z_d, and Γ_d over the range 0–10 GHz for the active element with the tuning and terminating open stubs.

It is seen that the negative resistance at the oscillator output port

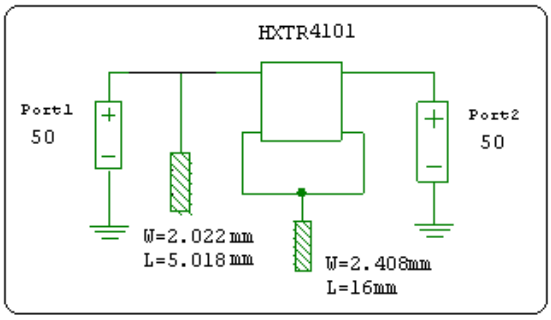

Figure 6. Aplac configuration of the active element with the tuning and terminating open stubs at its base and emitter terminals.

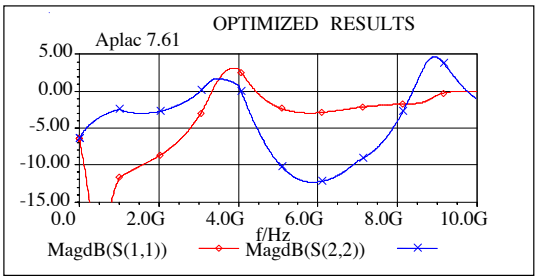

Figure 7. $|S_{11}|$ and $|S_{22}|$ versus frequency for the HXTR-4101 BJT with tuning and terminating stubs at its base and emitter terminals.

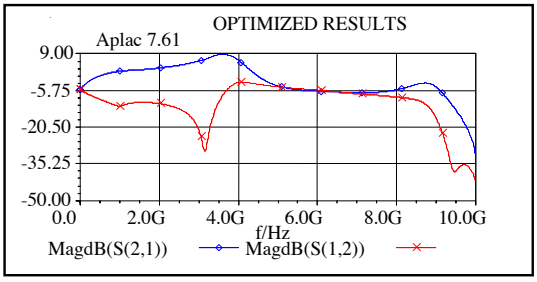

Figure 8. $|S_{21}|$ and $|S_{12}|$ versus frequency for the HXTR-4101 BJT with tuning and terminating stubs at its base and emitter terminals.

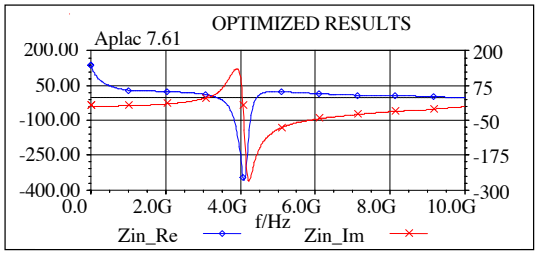

Figure 9. Real and imaginary parts of Z_d versus frequency for the HXTR-4101 BJT with tuning and terminating stubs at its base and emitter terminals.

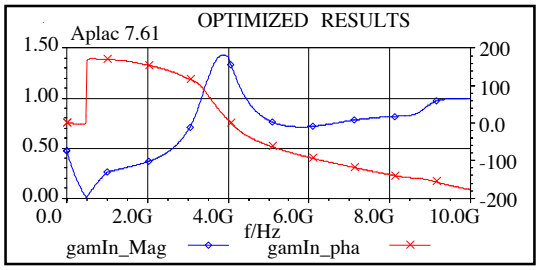

Figure 10. Magnitude and phase parts of Γ_d versus frequency for the HXTR-4101 BJT with tuning and terminating stubs at its base and emitter terminals.

exists over the bandwidth extends from 3.3 to 4.4 GHz. It is also seen that Γ_d is greater than 1 over this range. The value of device impedance Z_d at the operating frequency is $-360 - j268.3\,\Omega$.

To achieve a good output power of the oscillator, the negative resistance looking into the collector is designed to be near three times that of the resistance looking into the output load, i.e.,

$$-\mathrm{Re}[Z_d] \approx 3\mathrm{Re}[Z_L] \tag{5}$$

According to the value of Z_d, the optimum value of Z_L is selected to be $120 + j268.3$.

The fourth step is to design analytically and optimize the proper matching circuit at the oscillator output so that a 50 ohm load can be derived. The oscillator output matching circuit is designed using the developed simulation program. The parameters of the output matching circuit are shown in Table 3. Figures 11 and 12 show the Aplac configuration and the microstrip schematic diagram of the designed negative resistance oscillator operated at 4 GHz.

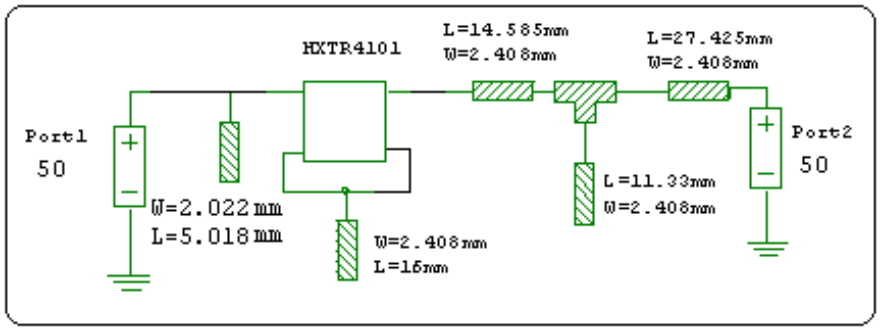

Figure 11. The Aplac configuration of the designed negative resistance oscillator operated at 4 GHz.

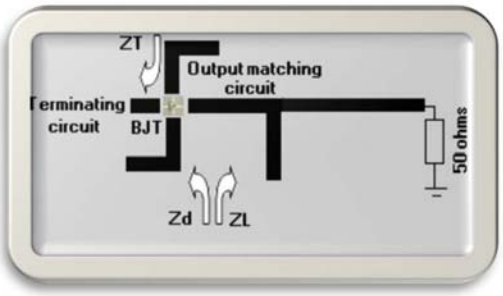

Figure 12. The microstrip schematic diagram of the designed negative resistance oscillator operated at 4 GHz.

Table 3. Parameters of the matching circuit at the collector terminal of the active element.

item	Length	Width
Series microstrip line	14.584 mm	2.408 mm
Open circuit single stub	11.333 mm	2.408 mm

3. DESIGN OF THE MICROSTRIP PATCH ANTENNA

A microstrip patch antenna (MPA) consists of a conducting patch of any planar geometry on one side of a dielectric substrate backed by a ground plane on the other side [2–4, 20]. Such antennas received considerable attention starting in 1970s [3] and are used now to

implement hybrid MIC and MMIC transceiver modules [5]. There are numerous substrates that can be used for the design of microstrip antennas, and their dielectric constants are usually in the range of ($2.2 \leq \varepsilon_r \leq 12$). The substrates that are most desirables for antenna performance are thick ones whose dielectric constants are in the lower end of the range. This provides better efficiency, larger bandwidth, and loosely bound fields for radiation into space, but at the expense of larger element size. On the other hand, the microwave circuit attached to the antenna requires thin substrate with high dielectric constant since this ensures tightly bound fields. Hence the undesired radiation and coupling can be minimized. In addition the microwave circuit size can be reduced.

Since microstrip antennas are integrated with the circuit in our module, a compromise has to be reached between good antenna performance and circuit design. The microstrip substrate whose parameters are given in the previous section was found to represent the optimum compromise.

The negative resistance of the oscillator is tuned to $50\,\Omega$ interface through the oscillator output matching circuit. To enhance the performance of the inset-fed MPA, the $50\,\Omega$ interface of the negative-resistance oscillator and the hybrids should be matched to the onput impedance of antenna through the proper values of the inset distance and width.

A computer program is developed in order to design the MPA and to calculate its parameters. The equations used in the program are based on using the transmission-line model for the antenna [2, 21–23]. The E- and H-plane patterns are based on using the cavity model [2]. These equations are summarized as follows:

1) The width (w) of the patch antenna is given by:

$$w = \frac{\lambda}{2}\left(\frac{\varepsilon_r + 1}{2}\right)^{-\frac{1}{2}} \tag{6}$$

Where: λ is the free-space wavelength. The width was found to be 26.35 mm.

2) The effective dielectric constant ε_{reff} is given by:

$$\varepsilon_{reff} = \frac{\varepsilon_r + 1}{2} + \frac{\varepsilon_r - 1}{2}\left[1 + 12\frac{h}{w}\right]^{-1/2} \tag{7}$$

3) The length of the MPA is given by:

$$L = \frac{\lambda_g}{2} - 2\Delta l \tag{8}$$

Where:

$$\Delta l = 0.412h\frac{(\varepsilon_{reff}+0.3)\left(\frac{w}{h}+0.264\right)}{(\varepsilon_{reff}-0.258)\left(\frac{w}{h}+0.8\right)} \tag{9}$$

The length was found to be 22.09 mm.

4) If the coordinate system illustrated in Figure 13 is used, the E-plane radiation pattern is given by [2]:

$$E_\Phi = j\frac{kwV_o}{\pi r}e^{-jkr}\left[\frac{\sin\left(\frac{kh}{2}\sin\Phi\right)}{\frac{kh}{2}\cos\Phi}\right]\cos\left(\frac{kL_e}{2}\sin\Phi\right) \tag{10}$$

and the H-plane radiation pattern is given by:

$$E_\Theta = j\frac{kwV_o}{\pi r}e^{-jkr}\left[\sin\Theta\frac{\sin\left(\frac{kh}{2}\sin\Theta\right)\sin\left(\frac{kw}{2}\cos\Theta\right)}{\frac{kh}{2}\sin\Theta\frac{kw}{2}\cos\Theta}\right] \tag{11}$$

Where: $k=\frac{2\pi}{\lambda}$, V_o is the amplitude of the applied voltage of the signal, and L_e is the effective length of the antenna given by $L_e = L + 2\Delta l$.

5) The radiation resistance (R_r) is given by:

$$R_r = \frac{1}{2G_1} \tag{12}$$

Where:

$$G_1 = \frac{I_1}{120\pi^2} \tag{13}$$

and

$$I_1 = \int_0^\pi \sin^2\left(\frac{kw\cos\theta}{2}\right)\tan^2\theta\sin\theta d\theta \tag{14}$$

6) The directivity D is given by:

$$D = \left(\frac{2\pi w}{\lambda}\right)^2\frac{1}{I_1} \tag{15}$$

The effective gain is given by:

$$G = \eta D \tag{16}$$

Where: η is the antenna efficiency.

7) The bandwidth is given by:

$$BW = 3.77\frac{\varepsilon_r - 1}{\varepsilon_r^2}\frac{h}{\lambda} \tag{17}$$

The computed E- and H-plane patterns are given in Figures 14 and 15, respectively. The computed input resistance is 200 Ω [23]. The location of the feed is chosen at the middle of the patch side at which the feed line is connected. The theoretical directivity was 15.69 dB. The E- and H-plane beamwidths are 91.7° and 18.2°, respectively.

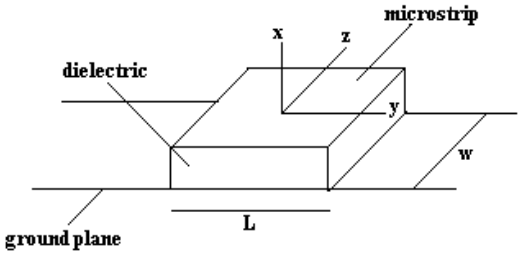

Figure 13. The microstrip-patch antenna and the coordinate system.

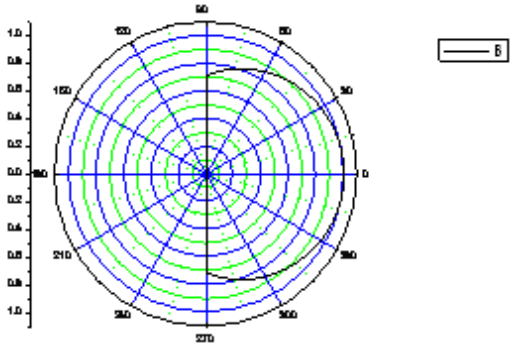

Figure 14. The calculated E-plane antenna pattern.

All the four-radiating elements of the antenna are identical and they are designed based on the rectangular patch antenna with inset feed. The separation between the adjacent elements is adjusted to the required E- and H-plane radiation patterns.

In order to improve the noise figure while maintain a good gain and conjugate match, the input impedance of the inset-fed MPA (Z_{in}) is adjusted to match with 50 Ω interface (hybrid output

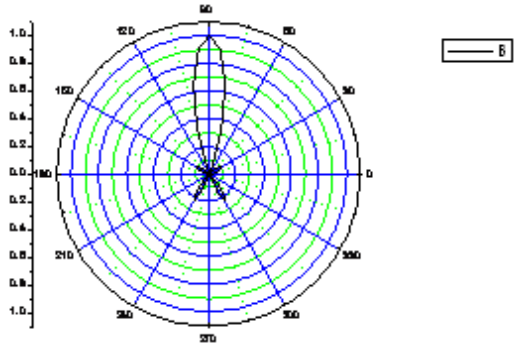

Figure 15. The calculated H-plane antenna pattern.

impedance and hence the output impedance of the negative resistance oscillator). The value of Z_{in} is usually in the range of 100–400 Ω. Since there is no formula to accurately calculate Z_{in} from the antenna parameters (L, W) and substrate parameters (ε_r, h, t) at the operating frequency, the value of Z_{in} at resonance is assumed to be 200 Ω and in accordance it will be transferred to 50 Ω interface through a set of $\lambda_g/4$ transformers.

The best excitation of the MPA is fed at its line of symmetry. Since Z_{in} mainly depends on the inset distance (y_o) and gaps between the fed line of the antenna (g), the values of y_o and g is tuned to get the proper value of Z_{in} (200 Ω).

4. DESIGN OF LANGE COUPLER

The balanced transmitter with coupled-line hybrid at the output of the oscillator has mainly two problems. The first one is that the required even and odd mode characteristic impedances of the coupler are beyond the manufacturing capability, even on high permittivity substrate, because the required spacing between the lines is too small. The second problem is that the two outputs emerge on opposite sides of the isolated ports, so a symmetrical circuit layout is difficult to achieve.

Lange coupler can be used to overcome these two problems. The developed full-scale computer simulation program and Aplac software are used to design and to optimize the Lange hybrid operated at central frequency of 4 GHz with four coupled lines ($N = 4$) and the coupling factor = 3 dB. Figure 16 shows the Aplac configuration of 4 GHz Lange coupler. As a result of the developed program and Aplac software, the parameters of the Lange hybrid are: strip separation

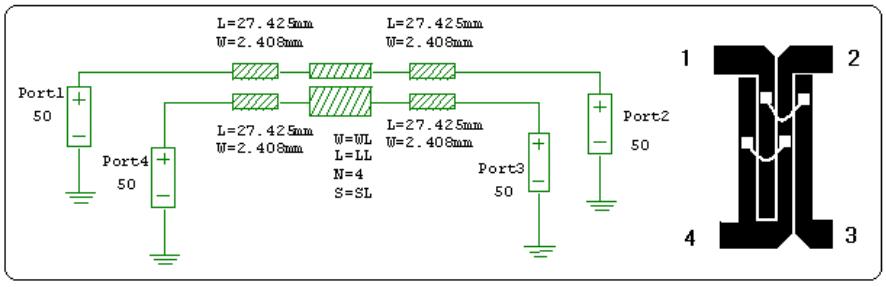

Figure 16. The Aplac configuration of the designed Lange coupler operated at 4 GHz: (1) Input port. (2) Coupled port. (3) Directed port and (4) Isolated port.

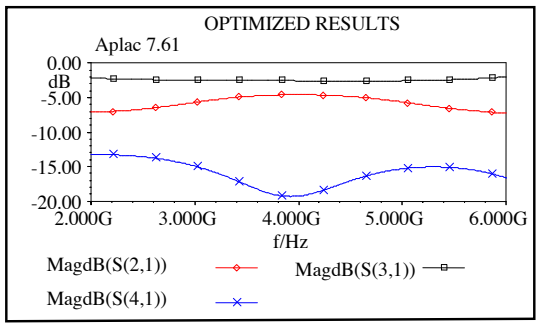

Figure 17. The optimized $|S_{21}|$, $|S_{31}|$, and $|S_{41}|$ versus frequency (GHz) for a Lange coupler operated at 4 GHz.

$(S) = 0.1\,\text{mm}$, strip width $(W) = 0.23\,\text{mm}$, even mode impedance $(Z_{oe}) = 176.4\,\Omega$, odd mode impedance $(Z_{oo}) = 52.5384\,\Omega$, even mode W/H ratio = 1.1589, odd mode W/H ratio = 7.29, and coupled line length $(L) = 14.362\,\text{mm}$. Figure 17 shows the optimized $|S_{21}|$, $|S_{31}|$, and $|S_{41}|$ versus frequency (GHz) for the Lange coupler operated at 4 GHz. Figure 18 shows optimized phase difference between coupled and directed ports of the Lange coupler.

5. DESIGN OF BRANCH COUPLERS

One or two-section branch line couplers can be used to split the oscillator output. The developed computer simulation program and Aplac V7.61 software are used for the design and analysis of one (two)-section branch coupler operated at 4 GHz.

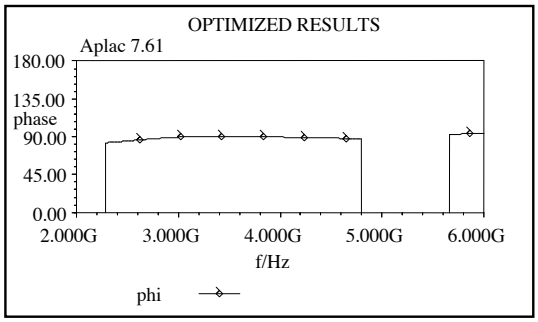

Figure 18. The optimized phase difference between coupled and directed ports of the Lange coupler.

5.1. One-section Branch Coupler

Table 4 illustrates the results for one-section branch line couple. Figure 19 shows the Aplac configuration of the designed one-section coupler operated at 4 GHz. Figure 20 shows the optimized $|S_{21}|$, $|S_{31}|$, and $|S_{41}|$ versus frequency (GHz) for the one-section branch coupler operated at 4 GHz. Figure 21 shows optimized phase difference between coupled and directed ports of the Lange coupler.

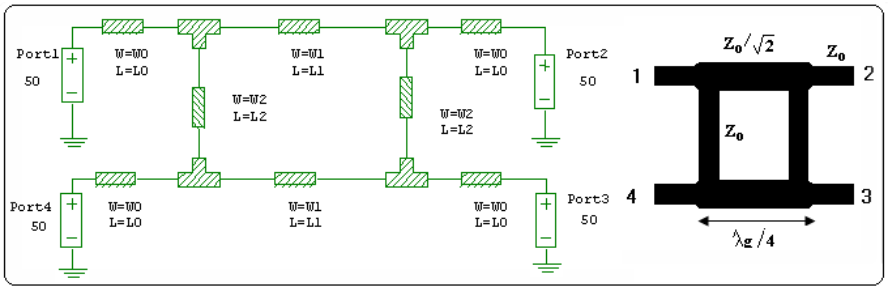

Figure 19. The Aplac configuration of the designed one-section branch coupler operated at 4 GHz: (1) Input port. (2) Coupled port. (3) Directed port and (4) Isolated port.

5.2. Two-section Branch Coupler

Table 5 illustrates the results for two-section branch coupler.

Figure 22 shows the Aplac configuration of the designed two-section coupler operated at 4 GHz. Figure 23 shows the optimized $|S_{21}|$, $|S_{31}|$, and $|S_{41}|$ versus frequency (GHz) for the two-section branch

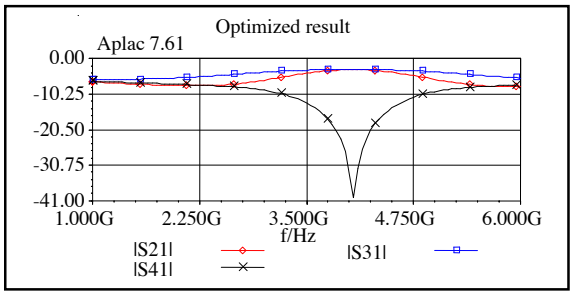

Figure 20. The optimized $|S_{21}|$, $|S_{31}|$, and $|S_{41}|$ versus frequency (GHz) for the one-section branch coupler operated at 4 GHz.

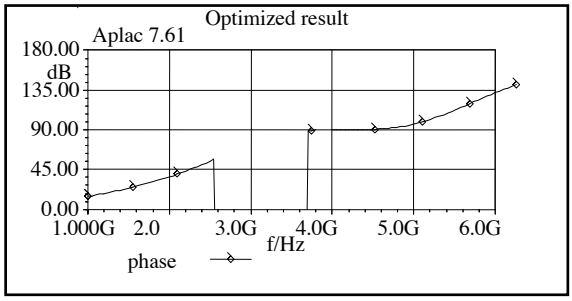

Figure 21. The optimized phase difference between coupled and directed ports of the one-section branch coupler.

Table 4. One-section branch line coupler.

	Series lines	Branch lines
Impedance	$35.3133\,\Omega$	$50\,\Omega$
Length	$L1 = 11.41$ mm	$L2 = 12.835$ mm
Width	$W1 = 3.762$ mm	$W2 = 2.351$ mm

coupler operated at 4 GHz. Figure 24 shows the optimized phase difference between coupled and directed ports of the two-section branch coupler operated at 4 GHz.

Figures 25 through 27 show the complete schematic diagrams of three 4 GHz transmitter modules using Lange, one-section branch and two-section branch couplers.

Table 5. Two-section branch coupler.

	Series lines	Branch (inside) lines	Branch (outside) lines
Impedance	35.3 Ω	35.3 Ω	120.7 Ω
Length	$L1 = 13.51$ mm	$L2 = 13.51$ mm	$L3 = 14.349$ mm
Width	$W1 = 3.993$ mm	$W2 = 3.993$ mm	$W3 = 0.438$ mm

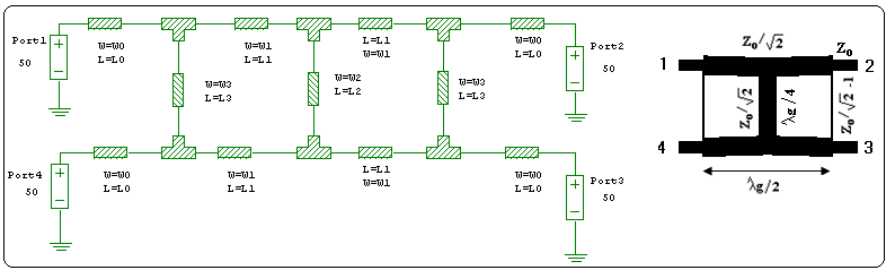

Figure 22. The Aplac configuration of the designed two-section branch coupler operated at 4 GHz: (1) Input port. (2) Coupled port. (3) Directed port and (4) Isolated port.

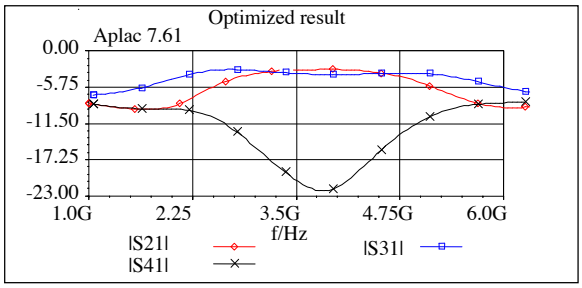

Figure 23. The optimized $|S_{21}|$, $|S_{31}|$, and $|S_{41}|$ versus frequency (GHz) for the two-section branch coupler operated at 4 GHz.

6. APPPLICATION AND FUTTURE WORKS

The designed integrated antenna modules have many applications including sensors, pulse Doppler communications, airborne radars, traffic control radars, satellite communications, etc.

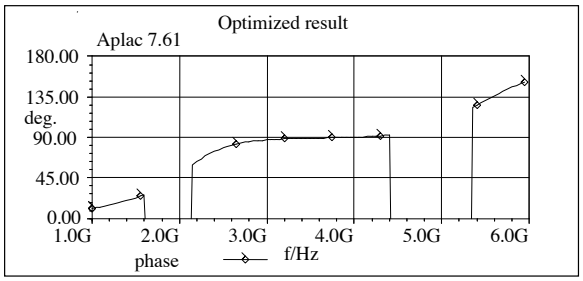

Figure 24. The optimized phase difference between coupled and directed ports of the two-section branch coupler.

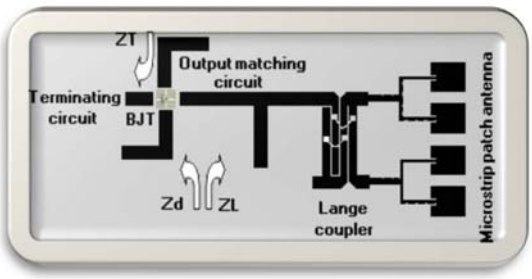

Figure 25. The complete schematic diagram of three 4 GHz transmitter modules using Lange coupler.

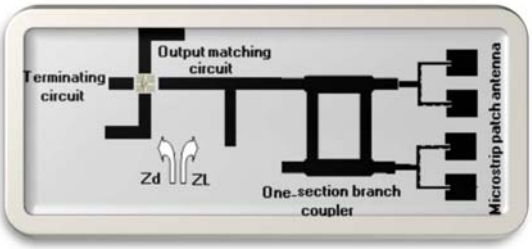

Figure 26. The complete schematic diagram of three 4 GHz transmitter modules using one-section branch coupler.

As a future work, the comparison between the performance of these modules will be studied with the effect of the bias networks in addition to a complete circuit simulation of the modules with all thier parts being connected (MPA, oscillator and coupler) using the most

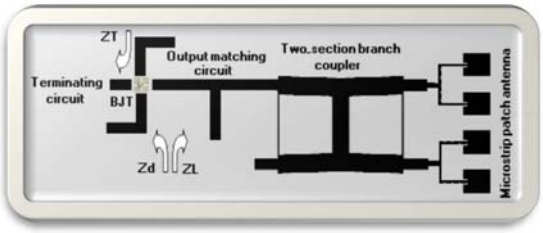

Figure 27. The complete schematic diagram of three 4 GHz transmitter modules using two-section branch coupler.

recent approaches for coupling FDTD with circuit functionality, device physics (drift-diffussion and hydrodynamic particle transportation) and the thermodynamic effects can be performed.

7. CONCLUSION

Three active integrated transmitter modules are designed and analyzed. These modules comprise a two-port-negative resistance oscillator operated at 4 GHz, and a patch antenna resonated at 4 GHz. The modules used Lange or branch (one or two sections) couplers to split the oscillator output. The modules are designed using the microstrip-line technology. The design methodologies of the two-port negative resistance oscillator and microstrip patch antenna are introduced and explained. The full scale-simulation program developed by the author is used for the design of the module elements. This simulation program fully takes into account all the discontinuities the microstrip design. The module elements are analyzed using Aplac V7.61 software. The analyses of the designed modules show a better efficiency and good performances. The modules give a transmit-antenna gain of 15.7 dB with antenna beam widths 91.7° and 18.2° in E- and H-planes, respectively. The complete schematic diagrams of the transmitter modules are drawn and the possible applications of these modules are illustrated.

REFERENCES

1. Itoch, T., "Quasi-optical microwave circuits for wireless applications," *Microwave J.*, Vol. 38, No. 1, 64–85, Jan. 1995.
2. Balanis, C. A., *Antenna Theory, Analysis and Design*, 2nd edition, John Wiley & Sons Inc., 1997.

3. Lee, K. F. and W. Chen, *Advances in Microstrip and Printed Antennas*, John Wiley & Sons Inc., 1997.
4. Cryan, M., P. Hall, S. Tsang, and J. Sho, "Integrated active antenna with full duplex operation," *IEEE Trans. on Microwave Theory & Tech.*, Vol. 45, No. 10, Oct. 1997.
5. Fusco, V., "Series feedback integrated active microstrip antenna synthesis and characterization," *Electron. Lett.*, Vol. 28, No. 1, Jan. 1992.
6. James, J. R. and P. S. Hall, *Handbook of Microstrip Antenna*, Peter Peregrinus, London, UK, 1989.
7. El-Motaafy, H., H. El-Hennawy, E.-S. El-Badawy, and S. H. Ibrahim, "A complete computer program for microstrip circuit design," *European Conference on Circuit Theory and Design (ECCTD-95)*, 27–31, Istanbul, Turkey, Aug. 1995.
8. Ibrahim, S. H., "A comprehensive CAD for microstrip, coaxial and waveguide circuits," *WSEAS Transactions on Electronics*, Vol. 4, No. 4, 91–100, May 2007,
9. Ibrahim, S. H., "Distributed MIC application for MSDES_WIN software," *WSEAS Transactions on Electronics*, Vol. 3, No. 11, 557–566, Nov. 2006.
10. Ibrahim, S. H., "Design and analysis of 4-GHz SOP FMCW HMIC radar," *WSEAS Transactions on Electronics*, Vol. 4, No. 4, 81–90, Apr. 2007.
11. Poza, D. M., *Microwave Engineering*, John Wiley & Sons Inc., 1998.
12. Collin, R. E., *Foundation for Microwave Engineering*, 2nd edition, McGraw-Hill Inc., 1992.
13. Edwards, T. C., *Foundations for Microstrip Circuit Design*, John Wiley & Sons Inc., 1992.
14. El-Motaafy, H. A., E. A. El-Badawy, and S. H. Ibrahim, "Effects of circuit and MESFET model parameters on the performance of microstrip oscillators," *ICME'96, the International Conference on Microelectronics*, Bandung, Indonesia, Jan. 16–17, 1996.
15. El-Motaafy, H. A., E. A. El-Badawy, and S. H. Ibrahim, "CAD program using a modified TD method and its application for the design and analysis of nonlinear MW active circuits," *PIERS'1997, Progress In Electromagnetic Research Symposium*, Kowloon, Hong Kong, Jan. 6–9, 1997.
16. El-Motaafy, H. A., M. M. El-Arabaty, and S. H. Ibrahim, "Design and realization of microwave oscillator and amplifiers using microstrip technology," *The XIII Conference on Solid-state*

Science, Sohag-Qena, Egypt, Jan. 20–26, 1990.

17. Ibrahim, S. H., E. A. El-Badawy, and H. A. El-Motaafy, "Computer-aided design of 2.6 GHz microstrip oscillator," *ICM'98*, Monastir, Tunisia, Dec. 14–16, 1998.
18. El-Badawy, E. A., H. A. El-Motaafy, and S. H. Ibrahim, "A complete computer program for microstrip circuit design," *ECCD'95, European Conference on Circuit Theory and Design*, Istanbul, Turkey, Aug. 27–31, 1995.
19. Woods, D., "Reappraisal of unconditional stability criteria for active 2-port network in terms of S-parameters," *IEEE Transaction on Circuits and Systems*, Feb. 1976.
20. El-Badawy, E. A., S. H. Ibrahim, and H. A. El-Motaafy, "Design and implementation of a 2-GHz active integrated antenna," *Symposium on Antenna Technology and Applied Electromagnetics, (ATNEM'2000)*, Winnipeg, Manitoba, Canada, Aug. 2, 2000.
21. Ramesh, M. and K. B. Yip, "Design formula for inset fed microstrip patch antenna," *Journal of Microwaves and Optoelectronics*, Vol. 3, No. 3, December 2003.
22. Murad, S. A. Z. and W. Ismail, "Design of active integrated antenna for dual frequency image rejection," *American Journal of Applied Sciences*, Vol. 3, No. 6, 1890–1894, 2006.
23. Bonefacic, D. and J. bartolic, "Design considerations of an active integrated antenna with negative resistance transistor oscillator," *Radioengineering*, Vol. 14, No. 4, December 2005.